

# Decay branching ratio $\Gamma_\alpha/\Gamma$ for the 4.033 MeV state in $^{19}\text{Ne}$ and the rate of the $^{15}\text{O}(\alpha, \gamma)^{19}\text{Ne}$ reaction in novae and accreting neutron stars

B. Davids,<sup>1</sup> A. M. van den Berg,<sup>1</sup> P. Dendooven,<sup>1</sup> F. Fleurot,<sup>1,\*</sup> M. Hunyadi,<sup>1</sup> M. A. de Huu,<sup>1</sup> K. E. Rehm,<sup>2</sup> R. E. Segel,<sup>3</sup> R. H. Siemssen,<sup>1</sup> H. W. Wilschut,<sup>1</sup> H. J. Wörtche,<sup>1</sup> and A. H. Wuosmaa<sup>2</sup>

<sup>1</sup>*Kernfysisch Versneller Instituut, Zernikelaan 25, 9747 AA Groningen, The Netherlands*

<sup>2</sup>*Physics Division, Argonne National Laboratory, Argonne IL 60439*

<sup>3</sup>*Department of Physics, Northwestern University, Evanston IL 60208*

(Dated: December 18, 2019)

The  $^{15}\text{O}(\alpha, \gamma)^{19}\text{Ne}$  reaction is one of two routes for breakout from the hot CNO cycles into the  $rp$  process in accreting neutron stars. Its astrophysical rate depends critically on the decay properties of excited states in  $^{19}\text{Ne}$  lying just above the  $^{15}\text{O} + \alpha$  threshold. We have measured the  $\alpha$ -decay branching ratios  $\Gamma_\alpha/\Gamma$  for these states using the  $p(^{21}\text{Ne}, t)^{19}\text{Ne}$  reaction at 43 MeV/u. Combining our measurements with previous determinations of  $\Gamma_\gamma$  for these states, we conclude that breakout from the hot CNO cycles into the  $rp$  process in novae is not possible, assuming current models accurately represent their temperature and density conditions.

PACS numbers: 98., 26.30.+k, 26.50.+x, 27.20.+n

Novae are thermonuclear runaways initiated by the accretion of hydrogen- and helium-rich material from stellar companions onto the surfaces of white dwarfs in binary systems. Energy production and nucleosynthesis in the hottest novae are determined principally by the CNO, NeNa, and MgAl cycles [1]. Under high temperature and density conditions, e.g. in accreting neutron stars, breakout from the hot CNO cycles into the  $rp$  process occurs [2], dramatically increasing the luminosity of outbursts and synthesizing nuclei up to masses of 100 u [3]. Several reactions have been suggested as pathways for this breakout [4], but only two are currently thought to be possibilities:  $^{15}\text{O}(\alpha, \gamma)^{19}\text{Ne}$  and  $^{18}\text{Ne}(\alpha, p)^{21}\text{Na}$ . The rate of the latter reaction is appreciable only at extreme temperatures and densities, such as are found in accreting neutron stars [4, 5, 6], while the former has been regarded as a more likely route in the relatively low temperature and density conditions in novae.

In astrophysical environments the  $^{15}\text{O}(\alpha, \gamma)^{19}\text{Ne}$  reaction proceeds predominantly through resonances lying just above the  $^{15}\text{O} + \alpha$  threshold at 3.529 MeV in  $^{19}\text{Ne}$ . The direct capture component is very small by comparison [7, 8]. The most important contribution to the resonant reaction rate in novae is made by the 4.033 MeV  $3/2^+$  state, owing both to its close proximity to the  $^{15}\text{O} + \alpha$  threshold and its low centrifugal barrier. The size of this contribution is essentially determined by the  $\alpha$ -width of the state,  $\Gamma_\alpha$ , which is much smaller than the  $\gamma$ -width  $\Gamma_\gamma$ . A previous attempt to determine  $\Gamma_\alpha$  for this state was based upon measurements of  $\alpha$ -transfer reactions to the analog state in the mirror nucleus  $^{19}\text{F}$  [9]. Such determinations, however, are subject to large uncertainties [10] and a measurement of  $\Gamma_\alpha$  in  $^{19}\text{Ne}$  itself is clearly indispensable for this important state.

At  $^{19}\text{Ne}$  excitation energies relevant to novae and accreting neutron stars, only the  $\alpha$ - and  $\gamma$ -decay channels are open, as the proton and neutron separation energies

are 6.4 and 11.6 MeV [11] respectively. Hence by populating these states and observing the subsequent  $\alpha$ - and  $\gamma$ -decays, one can deduce the branching ratio  $B_\alpha \equiv \Gamma_\alpha/\Gamma$ . If  $\Gamma_\gamma$  is also known, one can then deduce  $\Gamma_\alpha$  and thereby the contribution of each state to the resonant rate of  $^{15}\text{O}(\alpha, \gamma)^{19}\text{Ne}$ . A pioneering effort was made by detecting  $\alpha$  particles from the decay of  $^{19}\text{Ne}$  states populated via the  $^{19}\text{F}(^3\text{He}, t)^{19}\text{Ne}$  reaction [12], but the sensitivity of the experiment was insufficient to measure  $B_\alpha$  for the most important 4.033 MeV state, which was expected to be of order  $10^{-4}$ .

In an experiment at the Kernfysisch Versneller Instituut, we have carried out a measurement of the branching ratios  $\Gamma_\alpha/\Gamma$  for all states in  $^{19}\text{Ne}$  relevant to the  $^{15}\text{O}(\alpha, \gamma)^{19}\text{Ne}$  reaction in novae and accreting neutron stars. This determination was made using the  $p(^{21}\text{Ne}, t)^{19}\text{Ne}$  reaction at a bombarding energy of 43 MeV/u, detecting the  $^{19}\text{Ne}$  recoils and  $^{15}\text{O}$  decay products in coincidence with tritons in the Big-Bite Spectrometer (BBS) [13]. The large momentum acceptance of the BBS ( $\Delta p/p = 19\%$ ) allowed simultaneous detection of both  $^{19}\text{Ne}$  recoils or  $^{15}\text{O}$  decay products and tritons emitted backward in the center of mass system. Positioning the BBS at  $0^\circ$  maximized the yield to the 4.033 MeV  $3/2^+$  state in  $^{19}\text{Ne}$ . This state, whose dominant shell model configuration is  $(sd)^5(1p)^{-2}$  [14], was selectively populated by an  $\ell = 0$ , two-neutron transfer from the  $3/2^+$  ground state of  $^{21}\text{Ne}$ . Position measurements in two vertical drift chambers (VDCs) [15] allowed reconstruction of the triton trajectories. The excitation energies of the  $^{19}\text{Ne}$  residues were determined from the kinetic energies and scattering angles of the triton ejectiles. Branching ratios were obtained through the coincident detection of the heavy recoils and decay products. The  $\gamma$ -decays of states in  $^{19}\text{Ne}$  were observed as  $^{19}\text{Ne}$ -triton coincidences in the BBS, whereas  $\alpha$ -decays were identified from  $^{15}\text{O}$ -triton coincidences.

The residual heavy ions were detected and stopped just in front of the BBS focal plane by fast plastic-slow plastic phoswich detectors [16] that provided energy loss and total energy information. A separate array of phoswich detectors was used to identify tritons after they passed through the VDCs. Timing relative to the 31 MHz cyclotron RF signal was also employed for unambiguous particle identification. An Al plate was placed between the heavy-ion phoswich detectors and the VDCs in order to prevent the heavy ions copiously produced by projectile fragmentation reactions of the  $^{21}\text{Ne}$  beam in the  $\text{C}_2\text{H}_4$  target from reaching the VDCs. The spatial extent of the heavy-ion phoswich array was sufficient to guarantee 100% geometric efficiency for detection of the  $^{19}\text{Ne}$  recoils and  $^{15}\text{O}$  decay products for  $^{19}\text{Ne}$  excitation energies  $\leq 5.5$  MeV. This resulted from the forward focusing of the  $^{19}\text{Ne}$  recoils, which emerged at angles  $\leq 0.36^\circ$  for tritons with scattering angles  $\leq 4^\circ$ , and the low decay energies of the states studied, which limited the angular and energy spreads of the  $^{15}\text{O}$  decay products.

The  $^{19}\text{Ne}$  excitation energy spectrum obtained from  $^{19}\text{Ne}$ -triton coincidences, representing  $\gamma$ -decays of states in  $^{19}\text{Ne}$ , is shown in Fig. 1. The most prominent peak is due to the 4.033 MeV  $3/2^+$  state. The 4.379 MeV  $7/2^+$  state is the second most strongly populated. Contributions from other known states [17] are indicated. The experimental resolution of 87 keV FWHM is insufficient to resolve the 4.140 and 4.197 MeV states from one another; the 4.549 and 4.600 MeV states are also unresolved. However, the astrophysically important 4.033 and 4.379 MeV states are well separated from the others. A small background can be seen, e.g. in the gap between the 2.795 and 4.033 MeV states. The curve shown in Fig. 1 is the sum of a constant background and nine Gaussians centered at the well-known energies of the states, with  $\sigma = 37$  keV fixed by the experimental resolution of 87 keV FWHM.

Fig. 2 shows the  $^{19}\text{Ne}$  excitation energy spectrum obtained from  $^{15}\text{O}$ -triton coincidences, corresponding to  $\alpha$ -decays of states in  $^{19}\text{Ne}$ . The observed states are labeled by their energies; the 4.549 and 4.600 MeV states cannot be resolved. A fit of ten Gaussians plus a linear background is shown as well. The states below 4.6 MeV decay overwhelmingly by  $\gamma$ -emission, while the higher-lying states observed here decay preferentially by  $\alpha$ -emission, simply because the larger available decay energy enhances the barrier penetrability. The background represents a larger fraction of the total events in the  $^{15}\text{O}$ -triton coincidence spectrum than in the  $^{19}\text{Ne}$ -triton coincidence spectrum. Projectile fragmentation reactions in the target can produce  $^{15}\text{O}$  and tritons, mimicking the  $p(^{21}\text{Ne}, t)^{19}\text{Ne}$  reaction with subsequent  $\alpha$ -decay. However, fragmentation of  $^{21}\text{Ne}$  cannot produce  $^{19}\text{Ne}$  and a triton. Hence the background in the  $^{19}\text{Ne}$ -triton coincidence spectrum is due to random coincidences alone, while that in the  $^{15}\text{O}$ -triton coincidence spectrum also has a component due to real coincidences induced by pro-

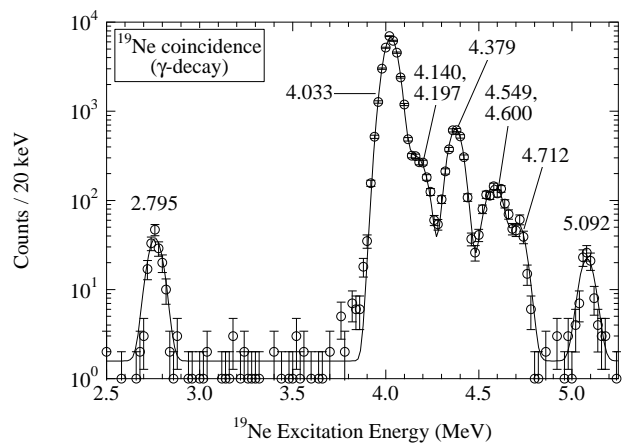


FIG. 1:  $^{19}\text{Ne}$ -triton coincidences ( $\gamma$ -decays of states in  $^{19}\text{Ne}$ ). The curve is the sum of a constant background and nine Gaussians corresponding to known states in  $^{19}\text{Ne}$  [17], the widths of which were determined by the experimental resolution of 87 keV FWHM.

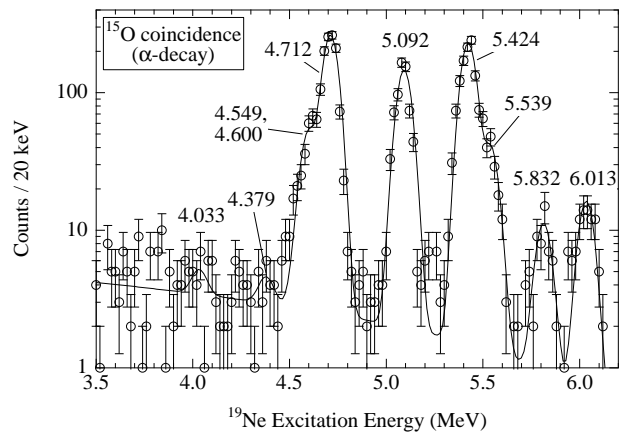


FIG. 2:  $^{15}\text{O}$ -triton coincidences ( $\alpha$ -decays of states in  $^{19}\text{Ne}$ ). The curve is the sum of a linear background and ten Gaussians corresponding to known states in  $^{19}\text{Ne}$ , the widths of which were fixed by the experimental resolution. The  $^{15}\text{O} + \alpha$  threshold lies at 3.529 MeV.

jectile fragmentation. This fragmentation background is well described by a linear function of excitation energy; its contribution to the fit shown in Fig. 2 is readily apparent in the range from 3.5-3.9 MeV, where there are no known states in  $^{19}\text{Ne}$ . The negative slope is a consequence of the position of the maximum of the triton fragmentation distribution, which lies at a large magnetic rigidity corresponding to a low  $^{19}\text{Ne}$  excitation energy. Here we see the low-energy tail of the triton fragmentation distribution.

Branching ratios for the various states were determined as follows. For the three well separated states where both  $\alpha$ - and  $\gamma$ -decay are energetically allowed, lying at 4.033, 4.379, and 5.092 MeV, the background-subtracted  $^{15}\text{O}$ -

triton coincidence and  $^{19}\text{Ne}$ -triton coincidence spectra were numerically integrated in  $\pm 50$  keV intervals centered at the known energies of the states, yielding  $N_\alpha$  and  $N_\gamma$  respectively. The branching ratio is then simply given by  $B_\alpha = \frac{N_\alpha}{N_\alpha + N_\gamma}$ . For the states at 4.549, 4.600, and 4.712 MeV that were not entirely resolved,  $B_\alpha$  was calculated using the fits described above. The branching ratios are shown in Table I along with the results of Ref. [12] and Ref. [18]. Uncertainties in the present branching ratio determinations are purely statistical. There is no indication in the data of  $\alpha$ -decays from the 4.140 and 4.197 MeV states. These decays are hindered by an  $\ell = 4$  centrifugal barrier and low decay energy. Small excesses above the background in the  $^{15}\text{O}$ -triton coincidence spectrum are evident at 4.033 MeV and 4.379 MeV. Our measurement of  $B_\alpha$  for the 4.379 MeV state is a factor of 17 smaller than the measurement of Ref. [12], a discrepancy we attribute to imperfect background subtraction in the previous determination. To obtain the resonance strengths we take a weighted average of  $B_\alpha$  where more than one measurement is available. The adopted values are shown in Table I.

The experimental data on  $\Gamma_\gamma$  for states in  $^{19}\text{Ne}$  are sparse. Of the six states considered here, measurements are available only for the 4.033 MeV state. The value adopted for this state [19] is the result of a combined analysis of Coulomb excitation and Doppler shift attenuation [20] data using shell model calculations of the relative strengths of E2 and M1 transitions. In some cases, widths of the analog state from the mirror nucleus  $^{19}\text{F}$  have been measured, and we adopt these under the assumption that  $\Gamma_\gamma(^{19}\text{Ne}) = \Gamma_\gamma(^{19}\text{F})$ . Such measurements are available for the 4.549 [17], 4.600 [21], and 4.712 MeV states [17]. For the 4.379 and 5.092 MeV states, measurements in neither nucleus are available, and we adopt the results of shell model calculations [22], assigning a 20% uncertainty to the calculated widths. The values of  $\Gamma_\gamma$  and  $\Gamma_\alpha$ , which is calculated as  $\Gamma_\alpha = \frac{B_\alpha}{1 - B_\alpha} \Gamma_\gamma$ , are shown in Table I. Our determination of  $\Gamma_\alpha$  for the crucially important 4.033 MeV state is a factor of 4 smaller than the weighted average of the two values given in Ref. [9] from measurements of  $\alpha$ -transfer reactions to the analog state in  $^{19}\text{F}$ .

Using these new widths, we calculate the thermally averaged reaction rates due to the six isolated, narrow resonances (e.g., [23]). The individual rates and the sum of the resonant and direct capture contributions are shown in Fig. 3. The direct capture rate was calculated as in Ref. [7], and is significant only below 0.1 GK. The contribution of the 4.033 MeV state, which is now based on direct experimental measurements, is seen to completely dominate the reaction rate for  $T \leq 0.5$  GK. The 4.600 and 4.712 MeV states account for most of the reaction rate at the high temperatures of 1.9 GK found in accreting neutron stars [3].

The  $^{15}\text{O}(\alpha,\gamma)^{19}\text{Ne}$  reaction leads to breakout from the

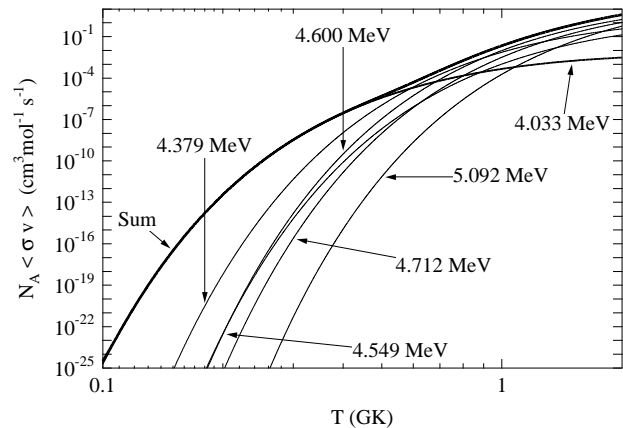


FIG. 3: Product of the Avogadro constant  $N_A$  and the thermally averaged rate of the  $^{15}\text{O}(\alpha,\gamma)^{19}\text{Ne}$  reaction. Contributions from all of the important resonances are shown, along with the sum of the resonant and direct capture rates.

hot CNO cycles if its rate is comparable to or greater than the  $\beta^+$  decay rate of  $^{15}\text{O}$  ( $t_{1/2} = 122$  s). In order to calculate the reaction rate in a particular environment one needs to know the local He mass fraction  $Y$ . We assume here a  $Y$  of 0.27, which is the solar value [24] adopted in accreting neutron star models [3], but is approximately twice the maximum value used in nova models [25, 26, 27]. Although the accreted material in novae is usually assumed to be of solar composition, significant mixing with the surface material of the white dwarf occurs prior to the nova outburst [28], rendering the net  $Y$  smaller than that of the accreted matter. Thus the rate we calculate with this  $Y$  represents an upper limit for novae. Fig. 4 shows the boundary in the density-temperature plane at which the rate of the  $^{15}\text{O}(\alpha,\gamma)^{19}\text{Ne}$  reaction equals the  $\beta^+$  decay rate of  $^{15}\text{O}$  for a  $Y$  of 0.27. Also shown are shaded regions corresponding to the peak temperatures and densities reached in nova outbursts and accreting neutron stars. The density we calculate agrees roughly with the estimate of Ref. [29], but is approximately 100 times greater than those of Ref. [2] and Ref. [12].

The extreme temperature and density conditions required to effect any appreciable flow out of the hot CNO cycles into the  $rp$  process via  $^{15}\text{O}(\alpha,\gamma)^{19}\text{Ne}$  are far beyond those encountered in current nova models, in which peak temperatures are typically 0.3 GK and densities  $10^3$ - $10^4$  g cm $^{-3}$  [25, 26, 27]. Since the rate of the  $^{18}\text{Ne}(\alpha,p)^{21}\text{Na}$  reaction appears too small in novae to compete with  $^{18}\text{Ne}$   $\beta^+$  decay [4, 5, 6], we conclude that breakout from the hot CNO cycles into the  $rp$  process in novae is precluded given our current knowledge of reaction rates and nova physics.

In summary, we have measured the  $\alpha$  branching ratios for all of the states in  $^{19}\text{Ne}$  relevant to the astrophysical rate of the  $^{15}\text{O}(\alpha,\gamma)^{19}\text{Ne}$  reaction, populating them by

TABLE I: Branching Ratios  $B_\alpha \equiv \Gamma_\alpha/\Gamma$  and Decay Widths

$E_x$ (MeV)	$J^\pi$	$B_\alpha$ (present work)	$B_\alpha$ (Ref. [12])	$B_\alpha$ (Ref. [18])	$B_\alpha$ (adopted)	$\Gamma_\gamma$ (meV)	Ref.	$\Gamma_\alpha$ (meV)
4.033	$\frac{3}{2}^+$	$2.4 \pm 1.9 \times 10^{-4}$			$2.4 \pm 1.9 \times 10^{-4}$	$12^{+9}_{-5}$	[19]	$2.9^{+3.2}_{-2.6} \times 10^{-3}$
4.379	$\frac{7}{2}^+$	$2.6 \pm 2.0 \times 10^{-3}$	$0.044 \pm 0.032$		$2.8 \pm 2.0 \times 10^{-3}$	$458 \pm 92$	[22]	$1.3 \pm 0.9$
4.549	$(\frac{1}{2}, \frac{3}{2})^-$	$0.035 \pm 0.090$	$0.07 \pm 0.03$		$0.066 \pm 0.028$	$39^{+34}_{-15}$	[17]	$2.8^{+2.7}_{-1.7}$
4.600	$(\frac{5}{2}^+)$	$0.30 \pm 0.06$	$0.25 \pm 0.04$	$0.32 \pm 0.03$	$0.30 \pm 0.02$	$101 \pm 55$	[21]	$42 \pm 24$
4.712	$(\frac{5}{2}^-)$	$0.83 \pm 0.05$	$0.82 \pm 0.15$		$0.83 \pm 0.05$	$43 \pm 8$	[17]	$210 \pm 80$
5.092	$\frac{5}{2}^+$	$0.88 \pm 0.05$	$0.90 \pm 0.09$		$0.88 \pm 0.05$	$196 \pm 39$	[22]	$1500 \pm 700$

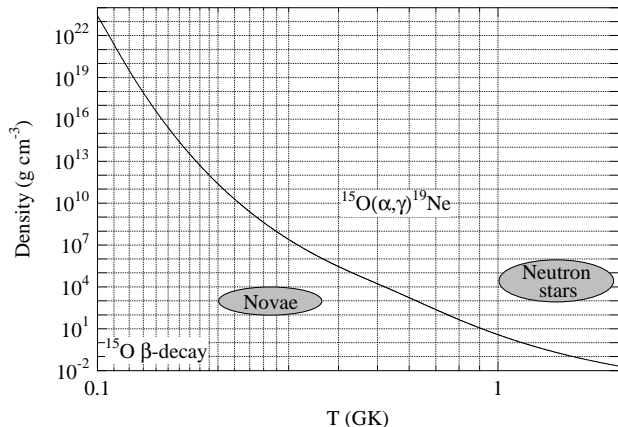


FIG. 4: Boundary in the density-temperature plane above which the rate of the  $^{15}\text{O}(\alpha,\gamma)^{19}\text{Ne}$  reaction exceeds the  $\beta^+$  decay rate of  $^{15}\text{O}$  for a He mass fraction of 0.27, the solar value. The shaded regions indicate the peak temperature and density conditions found in novae and accreting neutron stars.

means of the  $p(^{21}\text{Ne},t)^{19}\text{Ne}$  reaction at 43 MeV/u and observing their decays with 100% geometric efficiency in a magnetic spectrometer. Combining our measurements with prior determinations of the  $\gamma$ -widths of these states, we have calculated the astrophysical rate of  $^{15}\text{O}(\alpha,\gamma)^{19}\text{Ne}$  in novae and accreting neutron stars. For the first time, the calculation of the reaction rate at  $T \leq 0.5$  GK is based on direct experimental measurements. On the basis of these calculations and independent determinations of the  $^{18}\text{Ne}(\alpha,p)^{21}\text{Na}$  reaction rate, we conclude that there can be no breakout from the hot CNO cycles into the  $rp$  process in novae, assuming current models accurately represent their temperature and density conditions.

This work was performed as part of the research program of the *Stichting voor Fundamenteel Onderzoek der Materie* with financial support from the *Nederlandse Organisatie voor Wetenschappelijk Onderzoek*. KER, RHS, and AHW acknowledge support from a NATO Collaborative Linkage Grant. The ANL Physics Division is supported by the U. S. Department of Energy Nuclear Physics Division under Contract No. W-31-109-Eng38.

\* Present address: Department of Physics, Laurentian University, Sudbury ON, P3E 2C6, Canada

- [1] R. D. Gehrz et al., *Pub. Astron. Soc. Pac.* **110**, 3 (1998).
- [2] R. K. Wallace and S. E. Woosley, *Astrophys. J. Suppl. Ser.* **45**, 389 (1981).
- [3] H. Schatz et al., *Phys. Rev. Lett.* **86**, 3471 (2001).
- [4] M. Wiescher, J. Görres, and H. Schatz, *J. Phys. G* **25**, R133 (1999).
- [5] W. Bradfield-Smith et al., *Phys. Rev. C* **59**, 3402 (1999).
- [6] A. A. Chen et al., *Phys. Rev. C* **63**, 65807 (2001).
- [7] K. Langanke et al., *Astrophys. J.* **301**, 629 (1986).
- [8] M. Dufour and P. Descouvemont, *Nucl. Phys.* **A672**, 153 (2000).
- [9] Z. Q. Mao, H. T. Fortune, and A. G. Lacaze, *Phys. Rev. C* **53**, 1197 (1996).
- [10] F. de Oliveira et al., *Phys. Rev. C* **55**, 3149 (1997).
- [11] G. Audi and A. H. Wapstra, *Nucl. Phys.* **A595**, 409 (1995).
- [12] P. V. Magnus et al., *Nucl. Phys.* **A506**, 332 (1990).
- [13] A. M. van den Berg, *Nucl. Instrum. Methods* **B99**, 637 (1995).
- [14] H. T. Fortune, H. Nann, and B. H. Wildenthal, *Phys. Rev. C* **18**, 1563 (1978).
- [15] H. J. Wörtche et al., *Nucl. Phys.* **A687**, 321c (2001).
- [16] H. K. W. Leegte et al., *Nucl. Instrum. Methods* **A313**, 260 (1992).
- [17] D. R. Tilley et al., *Nucl. Phys.* **A595**, 1 (1995).
- [18] A. M. Laird et al., *Nucl. Phys.* **A688**, 134c (2001).
- [19] G. Hackman et al., *Phys. Rev. C* **61**, 052801 (2000).
- [20] J. M. Davidson and M. L. Roush, *Nucl. Phys.* **A213**, 332 (1973).
- [21] Á. Z. Kiss et al., *Nucl. Instrum. Methods* **203**, 107 (1982).
- [22] B. A. Brown, private communication (2002).
- [23] C. E. Rolfs and W. S. Rodney, *Cauldrons in the Cosmos* (The University of Chicago Press, Chicago, 1988).
- [24] E. Anders and N. Grevesse, *Geochim. Cosmochim. Acta* **53**, 197 (1989).
- [25] S. Wanajo, M.-A. Hashimoto, and K. Nomoto, *Astrophys. J.* **523**, 409 (1999).
- [26] S. Starrfield et al., *Astrophys. J. Suppl. Ser.* **127**, 485 (2000).
- [27] J. José, A. Coc, and M. Hernanz, *Astrophys. J.* **560**, 897 (2001).
- [28] R. Rosner et al., *Astrophys. J.* **562**, L177 (2001).
- [29] G. Vancraeynest et al., *Phys. Rev. C* **57**, 2711 (1998).